

Thermal Tomography of the Inner Regions of Protoplanetary Disks with the ngVLA and ALMA

Satoshi Okuzumi,¹ Munetake Momose,² and Akimasa Kataoka³

¹*Tokyo Institute of Technology, 2-12-1 Ookayama,
Meguro, Tokyo 152-8551*

²*Ibaraki University, 2-1-1 Bunkyo,
Mito, Ibaraki 310-8512*

³*National Astronomical Observatory of Japan, 2-21-1 Osawa,
Mitaka, Tokyo 181-8588
okuzumi@eps.sci.titech.ac.jp*

Abstract

Understanding the temperature structure of protoplanetary disks is crucial for answering the fundamental question of when and where in the disks rocky planets like our own form. However, the thermal structure of the inner few au of the disks is poorly understood not only because of lack of observational constraints but also because of the uncertainty of accretion heating processes. Here, we propose thermal tomography of the inner regions of protoplanetary disks with the ngVLA and ALMA. The proposed approach is based on the assumption that the inner disk regions are optically thick at submillimeter wavelengths but are marginally optically thin at longer millimeter wavelengths. By combining high-resolution millimeter continuum images from the ngVLA with submillimeter images at comparable resolutions from ALMA, we will be able to reconstruct the radial and vertical structure of the inner few au disk regions. We demonstrate that the thermal tomography we propose can be used to constrain the efficiency of midplane accretion heating, a process that controls the timing of snow-line migration to the rocky planet-forming region, in the few au regions of protoplanetary disks at a distance of 140 pc.

Key words: dust, extinction — planets and satellites: formation — protoplanetary disks — submillimeter: planetary systems — magnetohydrodynamics (MHD) — telescopes

1. Introduction

The temperature structure of protoplanetary disks dictates where planets of different compositions form in the disks. Rocky planets including the Earth are generally believed to have formed inside of the snow line, where the disk temperature reaches the sublimation temperature of water ice. Enhancement of solids outside the snow line due to ice condensation may help gas giants form within the lifetime of the gas disks (Kokubo & Ida, 2002). The composition of solids may even determine how planets form because the stickiness of solid particles generally depends on their surface composition (Chokshi et al., 1993).

Despite its importance in planet formation, the temperature structure of the inner regions of protoplanetary disks is poorly understood. Conventionally, the disk temperature structure has been studied based on the viscous accretion disk model that assumes vertically uniform viscosity. According to this classical disk model, accretion heating at the midplane pushes the midplane snow line in ~ 1 Myr-old disks out to 2–3 au (Davis, 2005; Garaud & Lin, 2007; Oka et al., 2011; Bitsch et al., 2015). However, the validity of the classical viscous model has been questioned by recent magnetohydrodynamical (MHD) simulations of protoplanetary disks showing that accretion heating can only take place near the disk surface, where the ionization fraction is relatively high (Hirose & Turner, 2011; Mori et al., 2019). A recent disk temperature model based on MHD simulations predicts that the snow line in ~ 1 Myr-old

disks must lie interior to 1 au (Mori et al., 2021). This raises the fundamental question of why the Earth is so dry with a bulk water content likely well below 1 wt% (Abe et al., 2000; Marty, 2012), because the solids outside the snow line in the solar nebula would have contained water ice in excess of 1 wt% as witnessed by carbonaceous chondrites and comets (e.g., van Dishoeck et al., 2014). In fact, simulations show that rocky planetary embryos at 1 au are likely to grow into waterworlds if the snow line migrates inward of the 1 au orbit within 1 Myr after disk formation (Sato et al., 2016) unless some mechanism stops the inward migration of the icy dust particles (e.g., Morbidelli et al., 2016).

To summarize, constraining the thermal structure of the inner regions of protoplanetary disks from astronomical observations is crucial for fully understanding how rocky planets form. In this article, we propose a methodology for testing disk temperature models by multi-wavelength, high-resolution imaging with the ngVLA and ALMA.

2. Theoretical Background

In principle, the efficiency of midplane heating can be studied by measuring disk temperatures at different vertical depths. In classical accretion disk models with vertically uniform kinematic viscosity, accretion heating mainly takes place at the midplane, leading to the midplane temperature higher than the surface temperature in inner disk regions (e.g., Davis, 2005). In contrast, in MHD accretion disk models, Joule heating takes

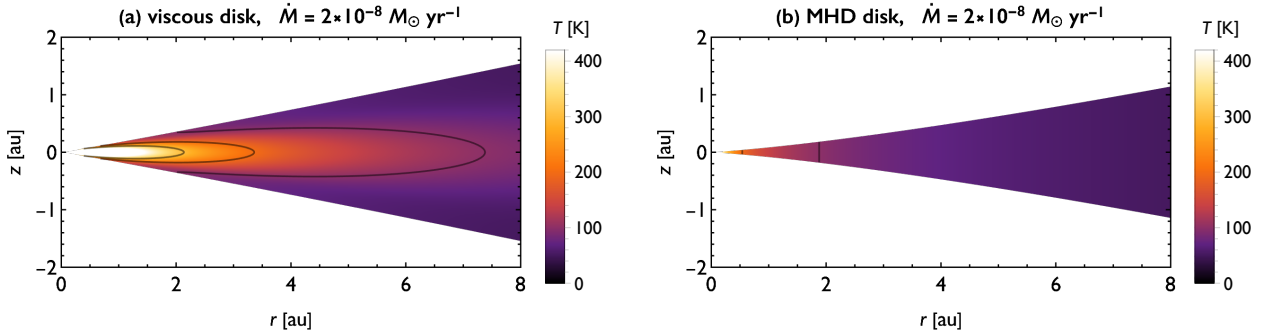


Fig. 1. Temperature as a function of the cylindrical radius r and distance from the midplane z for the viscous and MHD disks (panels (a) and (b), respectively). The contours mark $T = 100, 200,$ and 300 K. The maps are truncated at three scale heights below and above the midplane.

place well above the midplane, leading to vertically uniform temperature structure with the midplane no hotter than the surface (Hirose & Turner, 2011; Mori et al., 2019). This difference critically affects when the snow line crosses the 1 au orbit in the disks (Mori et al., 2021).

Multi-wavelength observations of the disks’ inner regions using the ngVLA and ALMA will enable us to perform thermal tomography—imaging of the temperature structure in both the radial and vertical directions—of the rocky planet-forming regions. The ngVLA will provide access to the midplane temperature structure of the inner few au of the disks at millimeter to centimeter wavelengths, at which the inner regions are likely to be optically marginally thick to optically thin. ALMA is already capable of mapping the dust continuum emission from well above the midplane at comparable resolutions at optically thick, submillimeter wavelengths.

3. Proof-of-concept Simulations

3.1. Models

We examine the feasibility of the disk thermal tomography described above using two disk temperature models. One is the classical viscous disk model (Lynden-Bell & Pringle, 1974) with the viscous alpha parameter α taken to be 10^{-3} throughout the disk. The other is the MHD accretion disk model recently proposed by Mori et al. (2021), which assumes accretion heating to occur on thin layers near the disk surfaces. For simplicity, we take the depth of the heating layers to be 0.4 g cm^{-2} in column mass density measured from infinity (Mori et al., 2019, 2021). The radial and vertical temperature profiles for the two accretion disk models are generated using the plane-parallel radiative transfer model by Hubeny (1990). In addition to accretion heating, we also include heating by stellar radiation (Chiang & Goldreich, 1997). For both models, we assume a uniform accretion rate of $\dot{M} = 2 \times 10^{-7} M_{\odot} \text{ yr}^{-1}$, a stellar mass of $1M_{\odot}$, a stellar luminosity of $1L_{\odot}$, and a uniform infrared opacity of $5.0 \text{ cm}^2 \text{ g}^{-1}$. Figure 1 shows the two-dimensional temperature maps for the two disk models.

The two-dimensional temperature profiles are used to generate maps of dust continuum emission from a face-on disk at submillimeter to centimeter wavelengths. The disk opacity in this wavelength range is assumed to follow a power law $\kappa(\lambda) = 6 \times 10^{-3} (\lambda/3 \text{ mm})^{-1.7} \text{ cm}^2 \text{ g}^{-1}$, where λ is the wavelength. Again, the opacity is taken to be uniform throughout the

disks, which means that we neglect possible spatial variations of the dust-to-gas mass ratio and grain size distribution due to dust evolution.

To mimic observations, Gaussian convolution is applied to smooth the theoretical continuum intensity profiles at angular resolutions of ALMA and the ngVLA. Specifically, we adopt angular resolutions of 12, 5, and 16 mas for the ALMA 0.87 mm, ngVLA 3 mm, and ngVLA 1 cm bands, respectively, estimated by Ricci et al. (2018) assuming 8 and 20 hr observations with ALMA and the ngVLA, respectively. The modeled disks are assumed to be located a distance of $d = 140$ pc away from the Earth, resulting in spatial resolutions of 1.7, 0.7, and 2.2 au for the 0.87 mm, 3 mm, and 1 cm band images, respectively. Based on the sensitivity estimates by Ricci et al. (2018), the rms noise in the brightness temperature maps for the three bands are estimated to be $\approx 0.6, 2,$ and 0.8 K. The sensitivities are high enough for a precise measurement of thermal emission from around the snow line, where $T \approx 160$ K.

3.2. Results

Figure 2 presents the maps of the brightness temperatures T_{B} at three wavelengths from the viscous disk model. The upper and lower panels are the maps before and after Gaussian smoothing, respectively. Comparison between the upper and lower panels shows that the angular resolutions of the ALMA submillimeter band and ngVLA millimeter bands are high enough to resolve the radial distribution of T_{B} in the inner few au. It is interesting to note that the brightness temperature of the inner disk region is maximized at $\lambda = 3$ mm and decreases both longward and shortward of 3 mm. This reflects the vertical thermal structure of the uniformly viscous disk, in which the temperature decreases as we go away from the midplane. At $\lambda = 0.87$ mm, the inner region is optically thick and the thermal emission comes from ≈ 2 scale heights above the midplane. At $\lambda = 3$ mm, the inner region is marginally optically thick and the thermal emission is dominated by the midplane. Longward of 3 mm, the inner region is optically thinner at longer wavelengths, and the brightness temperature of the region decreases with increasing λ . This demonstrates the importance of multi-wavelength observations using ALMA and the ngVLA in studying internal heating in the inner regions of protoplanetary disks.

Figure 3 is the same as Figure 2, but for the MHD accretion disk model. The brightness temperatures of the MHD

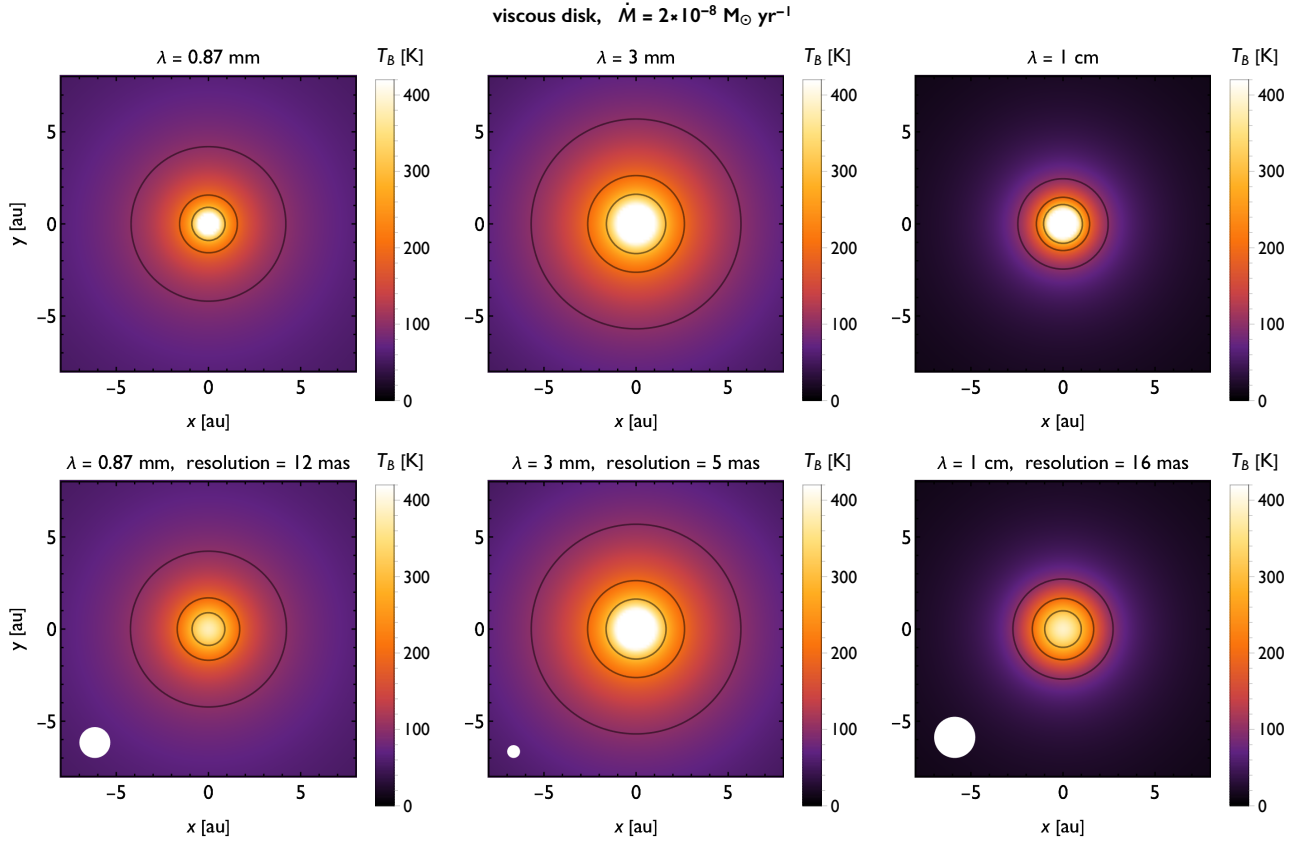


Fig. 2. Upper panels: maps of the brightness temperatures T_B at $\lambda = 0.87$ mm, 3 mm, and 1 cm (left, center, and right panels, respectively) from a face-on viscous accretion disk. The contours mark $T_B = 100, 200,$ and 300 K. Lower panels: synthetic brightness temperature maps after Gaussian smoothing, assuming $d = 140$ pc and spatial resolutions of 12, 5, and 16 mas for the ALMA 0.87 mm, ngVLA 3 mm, and ngVLA 1 cm bands, respectively (Ricci et al., 2018).

disk are overall lower than those of the viscous disk. Still, the synthetic map for the ngVLA 3 mm band accurately captures the brightness temperature profile of the MHD disk up to $T_B \approx 200$ K and thus allows us to study the thermal structure around the water snow line ($T \approx 160$ K). Because of its vertically uniform temperature structure, the MHD disk produces nearly identical brightness temperature maps (except for the unresolved very inner region) at optically thick wavelengths of $\lambda \lesssim 3$ mm. Therefore, multi-band observations at ALMA submillimeter bands and the ngVLA 3 mm band would allow us to test whether midplane heating is inefficient around the midplane in a disk.

4. Conclusion

We have demonstrated that thermal tomography with the ngVLA and ALMA will enable us to discriminate between different models for disk thermal structure. Such observations will provide us with a basis for fully understanding when and where terrestrial planets form. However, the models we have used here neglect a number of important dust evolution processes, including coagulation, vertical sedimentation, and radial drift. In particular, condensation, sublimation, and sintering of icy particles can significantly affect the size and spatial distribution of solids around the snow line (e.g., Birnstiel

et al., 2010; Ros & Johansen, 2013; Okuzumi et al., 2016; Schoonenberg & Ormel, 2017). All these dust evolution processes may alter the temperature structure and emission profiles in the inner regions of protoplanetary disks (e.g., Banzatti et al., 2015; Pinilla et al., 2017) and therefore should be included in future modeling.

5. Acknowledgments

We thank Takahiro Ueda for discussions. This work was supported by JSPS KAKENHI Grant Numbers JP18H05438, JP19K03926, JP19K03941, and JP20H00182.

References

- Abe, Y., Ohtani, E., Okuchi, T., Righter, K., & Drake, M. 2000, in *Water in the Early Earth, Origin of the Earth and the Moon*, eds. R. M. Canup, K. Righter, et al. (Tucson: University of Arizona Press), 413
- Banzatti, A., Pinilla, P., Ricci, L., et al. 2015, *ApJL*, 815, L15
- Birnstiel, T., Dullemond, C. P., & Brauer, F. 2010, *A&A*, 513, A79
- Bitsch, B., Johansen, A., Lambrechts, M., & Morbidelli, A. 2015, *A&A*, 575, A28
- Chiang, E. I., & Goldreich, P. 1997, *ApJ*, 490, 368

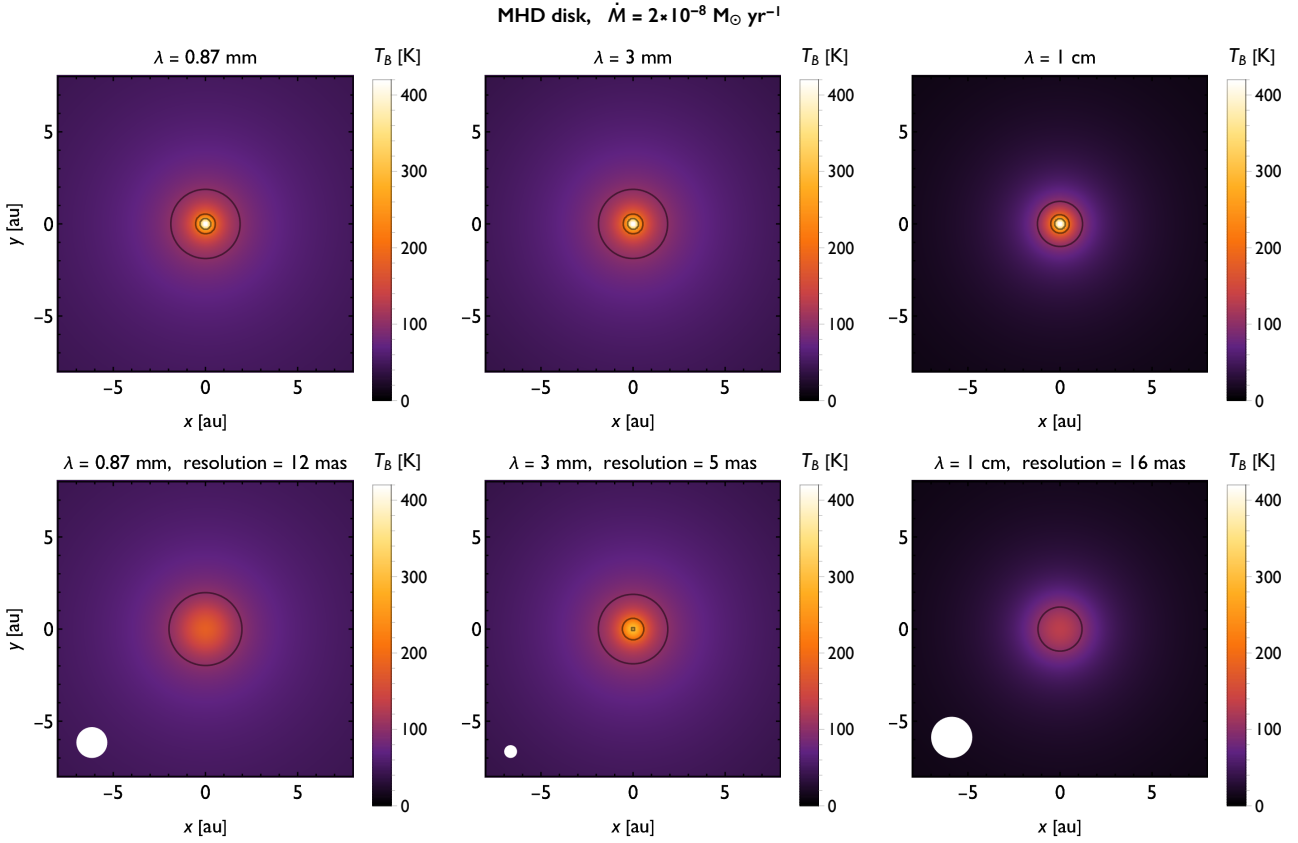


Fig. 3. Same as Figure 2 but for the MHD disk model.

- Chokshi, A., Tielens, A. G. G. M., & Hollenbach, D. 1993, *ApJ*, 407, 806
- Davis, S. S. 2005, *ApJ*, 620, 994
- Fernandes, R. B., Mulders, G. D., Pascucci, I., et al. 2019, *ApJ*, 874, 81
- Garaud, P., & Lin, D. N. C. 2007, *ApJ*, 654, 606
- Hirose, S., & Turner, N. J. 2011, *ApJL*, 732, L30
- Hubeny, I. 1990, *ApJ*, 351, 632
- Kokubo, E., & Ida, S. 2002, *ApJ*, 581, 666
- Lynden-Bell, D., & Pringle, J. E. 1974, *MNRAS*, 168, 603
- Marty, B. 2012, *Earth and Planetary Science Letters*, 313, 56
- Mori, S., Bai, X.-N., & Okuzumi, S. 2019, *ApJ*, 872, 98
- Mori, S., Okuzumi, S., Kunitomo, M., & Bai, X.-N. 2021, *ApJ*, 916, 72
- Oka, A., Nakamoto, T., & Ida, S. 2011, *ApJ*, 738, 141
- Okuzumi, S., Momose, M., Sirono, S.-i., Kobayashi, H., & Tanaka, H. 2016, *ApJ*, 821, 82
- Pinilla, P., Pohl, A., Stammer, S. M., & Birnstiel, T. 2017, *ApJ*, 845, 68
- Ros, K., & Johansen, A. 2013, *A&A*, 552, A137
- Sato, T., Okuzumi, S., & Ida, S. 2016, *A&A*, 589, A15
- Schoonenberg, D., & Ormel, C. W. 2017, *A&A*, 602, A21
- Morbidelli, A., Bitsch, B., Crida, A., et al. 2016, *Icarus*, 267, 368
- Ricci, L., Liu, S.-F., Isella, A., et al. 2018, *ApJ*, 853, 110
- van Dishoeck, E. F., Bergin, E. A., Lis, D. C., et al. 2014, *Protostars and Planets VI*, 835